Research Square

Preprints are preliminary reports that have not undergone peer review.
They should not be considered conclusive, used to inform clinical practice,
or referenced by the media as validated information.

Corneal biomechanical profiles and discriminative performance of pathological myopia with posterior staphyloma within a gradient myopia cohort Running title: Corneal biomechanical discrimination of posterior staphyloma in gradient myopia cohort

Xia Wang
Tianjin Eye Hospital
Yuxi Bai
Tianjin Medical University
Liyu Ren
Tianjin Eye Hospital
Huazheng Cao
Tianjin Eye Hospital
Siyuan Chen
Tianjin Medical University
Ying Wang
Tianjin Eye Hospital
Quanhong Han
hanquanhong126@126.com
Tianjin Medical University

Research Article

Keywords: High myopia, Posterior staphyloma, Corneal biomechanics, Corvis-ST

Posted Date: November 18th, 2026

DOI: https://doi.org/10.21203/rs.3.rs-11255442/v1

License: This work is licensed under a Creative Commons Attribution 4.0 International License. Read Full License

Additional Declarations: No competing interests reported.

Abstract

Purpose: To compare corneal biomechanical properties among moderate myopia (MM), simple high myopia (SHM), and pathologic myopia with posterior staphyloma (PM-PS); to explore the independent associations between corneal biomechanical parameters and posterior staphyloma; and to assess the incremental diagnostic value of these parameters beyond conventional models.

Methods: In this cross-sectional study, 147 myopic participants were categorized into MM (n = 49), SHM (n = 66), and PM-PS (n = 32) groups. Corneal biomechanical parameters were measured with Corvis ST. Analysis of covariance (ANCOVA), adjusted for age, axial length (AL), and central corneal thickness (CCT), was used to evaluate independent between-group effects. Receiver operating characteristic (ROC) curves, integrated discrimination improvement (IDI), and continuous net reclassification improvement (NRI) were used to evaluate discriminative performance and incremental value.

Results: In univariate analysis, multiple corneal biomechanical parameters differed significantly between groups; after adjustment for confounders, only DA Ratio Max 1 mm (P = 0.020) and A2 time (P = 0.037) remained significant, both increasing across MM < SHM < PM-PS. For A2 time, this pattern represented a reversal of the unadjusted trend. Individual biomechanical parameters showed limited discriminative power for PM-PS; adding A2 time and the stress-strain index (SSI) to a classical model based on AL and spherical equivalent (SE) significantly improved discrimination (AUC, 0.896 to 0.961; ΔAUC = 0.065, P = 0.005).

Conclusions: Most between-group differences in corneal biomechanics were attributable to confounding by age, AL, and CCT. DA Ratio Max 1 mm and A2 time were independently associated with posterior staphyloma. Individually, corneal biomechanical parameters had limited discriminative power; in combination, they provided incremental diagnostic value beyond conventional models based on axial length and refraction.

Introduction

Myopia is an important public-health concern with rising global prevalence[1]. Projections indicate that the global number of people with myopia will reach 4.758 billion by 2050, among whom 938 million will have high myopia (MH) [2]. HM may progress to pathological myopia (PM), which is defined by degenerative retinal changes secondary to axial elongation. Posterior staphyloma (PS), characterized by localized outward bulging of the posterior ocular wall, is one of its typical fundus manifestations[3, 4]. Abnormal scleral remodeling, scleral thinning and deteriorated mechanical properties participate in the development of PS in highly myopic eyes[5], which can lead to severe fundus complications including posterior-pole chorioretinal atrophy, macular hole and retinal detachment, and eventually irreversible visual loss. Therefore, risk stratification and disease monitoring for myopia are of great clinical significance.[6, 7]

PS is conventionally considered to occur exclusively in highly myopic eyes. Nevertheless, Xu et al. [8] reported PS in retinitis-pigmentosa patients with normal axial length (AL), suggesting that its pathogenesis is not merely attributed to axial elongation. The biomechanical properties of the entire ocular wall also deserve attention. The eye wall forms a continuous biomechanical complex. Although scleral biomechanics cannot be readily measured in-vivo, previous studies have demonstrated that the cornea and sclera share common extracellular-matrix origins[9]. Corneal biomechanical indices such as corneal hysteresis and corneal resistance factor are correlated with PS and regional scleral thickness[10]. Accordingly, corneal biomechanical parameters may indirectly reflect

scleral mechanical features. Corneal biomechanics describes the recoil characteristics of corneal tissue under external force[11]. The Corvis-ST is a Scheimpflug-based dynamic non-contact tonometer. It records real-time corneal deformation responses induced by an air-pulse stimulus and outputs deformation amplitude, applanation time, velocity, stress-strain index (SSI) and other derived metrics, enabling non-invasive in-vivo assessment of corneal biomechanics[12].

Previous studies have documented distinct Corvis-ST corneal biomechanical features in highly myopic versus non-highly myopic eyes, including augmented corneal deformation amplitude and modified viscoelastic behaviour, consistent with global ocular-wall remodeling in high myopia[12]. Sun et al. [13] demonstrated reduced corneal stiffness and enhanced deformability with higher refractive error and longer AL after adjustment for CCT and IOP. However, all high-myopia participants were pooled without stratification into PM and non-PM subgroups. Liao et al. [14] observed greater corneal deformation in PS eyes after AL adjustment and suggested an independent effect of PS on corneal biomechanics. Still, their analysis relied on a binary PS-versus-non-PS design without graded mild-to-moderate myopia controls. While several studies have performed severity-graded myopia comparisons, high-myopia subgroups were rarely stratified by PS status[13]. Insufficient adjustment for confounders (age, AL, CCT) in prior work further complicates discrimination between biomechanical changes secondary to axial elongation and intrinsic alterations driven by PS. Therefore, we utilised a three-tier myopia cohort (MM, SHM, PM-PS) to characterize PS-related corneal biomechanical profiles across the full spectrum of myopia severity.

In the present study, subjects were assigned to three groups: MM, simple high myopia (SHM), and pathological myopia with posterior staphyloma (PM-PS). After adjustment for age, AL and CCT, we aimed to explore whether PS produces corneal and corneoscleral biomechanical changes independent of axial elongation. Our results may supply clinical evidence for ocular-wall remodelling in PM and inform non-invasive clinical evaluation of PS.

Methods

This cross-sectional study consecutively enrolled myopic outpatients from Tianjin Eye Hospital. The study conducted in accordance with the tenets of the Declaration of Helsinki. Written informed consent was obtained from all participants.

Inclusion criteria was spherical equivalent (SE) ≤ − 0.5 D and absolute cylinder power ≤ 4 D. Exclusion criteria including history of corneal refractive surgery, keratoconus, corneal scarring, active ocular surface disease, glaucoma, ocular trauma or other disorders that may alter corneal biomechanics; retinal diseases other than high-myopia-related fundus lesions (e.g., diabetic retinopathy, retinal vascular occlusion, uveitis); patients with systemic comorbidities (e.g., diabetes, severe hypertension, autoimmune disease) or inability to complete examinations.

Participants were assigned into three groups according to SE and axial length (AL): (1) Moderate-to-moderate myopia group (MM): −6.00 D < SE ≤ − 0.50 D and AL < 26 mm; (2) Simple high myopia group (SHM): SE ≤ − 6.00 D or AL ≥ 26 mm, without PS or other pathological myopic changes; (3) PM with PS group (PM-PS): SE ≤ − 6.00 D or AL ≥ 26 mm, with PS confirmed by optical coherence tomography (OCT) and fundus photography.

All subjects underwent comprehensive ophthalmic examinations, including manifest refraction, best-corrected visual acuity (BCVA; converted to the logMAR scale using the Snellen chart), slit-lamp biomicroscopy, dilated fundus examination, ultra-wide-field swept-source OCT (SS-OCT; Saiwei, Henan, China), fundus photography (Carl Zeiss, Germany), anterior-segment biometry (Lenstar 900), and corneal biomechanical measurement (Corvis-ST).

Ocular biometry and anterior-segment parameter measurement: All examinations were performed by a single experienced technician. AL and mean corneal curvature (Km) were measured using Lenstar 900 (Haag-Streit AG, Switzerland). Each eye was measured in triplicate, and the mean value was adopted. The AL-to-corneal-radius ratio (AL/CR) was calculated using the formula: AL/CR = AL×Km/337.5 [15].

Corneal biomechanical assessment: Corneal biomechanical measurements were acquired with the Corvis-ST (Oculus Optikgeräte GmbH, Germany). This device is equipped with a high-speed camera and generates an air-pulse stimulus to induce corneal deformation, enabling real-time recording of dynamic corneal biomechanical responses[16]. The recorded parameters included: Stress-Strain Index (SSI), Stiffness Parameter at First Applanation (SP-A1), Maximum Deformation Amplitude Ratio at 2 mm (DA-Ratio-Max-2mm), Maximum Deformation Amplitude Ratio at 1 mm (DA-Ratio-Max-1mm), Integrated Radius (Integrated-Radius), Maximum Inverse Radius (Max-InverseRadius), Maximum Deflection Amplitude (Deflection-Amp-Max), Time at Maximum Deflection Amplitude (Deflection-Amp-Max-ms), Highest-Concavity Deformation Amplitude (HC-Deformation-Amp), Highest-Concavity Deflection Amplitude (HC-Deflection-Amp), First Applanation Time (A1-Time), First Applanation Velocity (A1-Velocity), Second Applanation Time (A2-Time), Second Applanation Velocity (A2-Velocity), Highest-Concavity Time (HC-Time), Peak Distance (Peak-Dist), Maximum Whole-Eye Movement (Whole-Eye-Movement-Max), Maximum Delta Arc Length (dArcLengthMax), Ambrosio Relational Thickness to the Horizontal Profile (ARTh). Only measurements with quality status “OK” were included. Each eye was tested three times, and the average value was calculated for further analysis.

Statistical Analysis

For each participant, only one eye was analyzed; for bilateral eligible eyes, the eye with posterior staphyloma was prioritized, and the right eye was selected when disease severity was comparable. Statistical analyses were performed using SPSS 26.0. The Anderson-Darling test was used to assess normality. Normally-distributed continuous variables were expressed as mean ± standard deviation (SD) and compared with independent-samples *t*-tests, while non-normal data were presented as median (P25, P75) and compared using the Mann-Whitney *U* test. Categorical variables were evaluated with the χ^2 test. One-way analysis of covariance (ANCOVA) was applied to assess independent inter-group effects after adjusting for age, AL and CCT with partial eta-squared (η^2) for effect-size estimation and estimated marginal means reported. The Bonferroni method was used for post-hoc pairwise comparisons, and ordinal-coded Spearman correlation was adopted for trend testing. Receiver operating characteristic (ROC) curves together with DeLong tests were used to evaluate discriminative performance for PM-PS versus non-PM-PS[17]. Classic (AL + SE) predictive models were constructed, and incremental diagnostic value of single or combined biomechanical parameters was quantified by ΔAUC, integrated discrimination improvement (IDI) and continuous net reclassification improvement (NRI) [18]. A two-sided $P < 0.05$ was defined as statistically significant.

Results

1. Baseline characteristics

Baseline demographic and anterior-segment parameters of the three groups are summarized in Table 1. A total of 147 eyes from 147 myopic patients were enrolled, including 49 eyes in the MM group, 66 eyes in the SHM group, and 32 eyes in the PM-PS group. Significant inter-group differences were observed in sex distribution and age (all $P < 0.001$). The PM-PS group had the highest proportion of female patients (81.3%), and age increased sequentially

following the order of MM to SHM to PM-PS. Statistically significant differences among groups were found for SE, AL and AL/CR (all $P < 0.05$), with values rising progressively from MM to SHM to PM-PS. No significant inter-group difference was detected for CCT ($P = 0.100$).

Table 1
Baseline demographic and anterior-segment characteristics of the three study groups.

Variable	MM (n = 49)	SHM (n = 66)	PM-PS (n = 32)	P value
Gender (famale, n%)	16(32.7%)*	45(67.2%)*	26(81.3%)	< 0.001
Age (years)	23(20,28)*	33(24.25,41)*	47(40.75,61)	< 0.001
Right eye, (n%)	19(38.8%)	35(53%)	15(46.9%)	0.318
SE(D)	−4.25(− 4.91,−3.34)*	−9.50(− 11.25,−8.00)*	−12.25(− 14.44,−9.88)	< 0.001
AL(mm)	25.46(25.00,25.84)*	27.18(26.36,27.98)*	28.80(27.90,29.53)	< 0.001
Km(D)	43.10 ± 1.07	43.96 ± 1.42	43.38 ± 1.31	0.002
AL/CR	3.23(3.19,3.29)*	3.55(3.44,3.64)*	3.65(3.59,3.85)	< 0.001
CCT(μm)	550.86 ± 30.85	537.41 ± 36.94	545.34 ± 28.82	0.100

*SE = spherical equivalent; AL = axial length; AL/CR = axial length-to-corneal radius ratio; Km = mean corneal curvature; CCT = central corneal thickness. *P < 0.05 vs. the PM-PS group.*

2 Inter-group differences of corneal biomechanics: univariate and adjusted analyses

2.1 Univariate inter-group comparisons

As shown in Table 2, significant inter-group differences were identified for multiple corneal biomechanical parameters in univariate analysis: Deflection-Amp-Max ($P = 0.007$), Max-InverseRadius ($P = 0.017$), SSI ($P = 0.017$), HC-Deflection-Amp ($P = 0.021$), DA-Ratio-Max-1mm ($P = 0.024$), HC-Deformation-Amp ($P = 0.028$), ARTh ($P = 0.028$), and A1-Time ($P = 0.042$). The remaining parameters did not differ significantly between groups (all $P > 0.05$; Supplementary Table S1).

Table 2
Univariate comparison of corneal biomechanical parameters across the three groups.

Variable	MM (n = 49)	SHM (n = 66)	PM-PS (n = 32)	P value
DA-Ratio-Max-1mm	**1.55 ± 0.04**	**1.58 ± 0.05**	**1.57 ± 0.05**	**0.024**
Max-InverseRadius(mm^{-1})	**0.16 ± 0.01**	**0.17 ± 0.02**	**0.17 ± 0.02**	**0.017**
Deflection-Amp-Max(mm)	**0.93 ± 0.07***	**0.97 ± 0.10**	**1.00 ± 0.10**	**0.007**
HC-Deformation-Amp(mm)	**1.08 ± 0.09***	**1.10 ± 0.11**	**1.14 ± 0.11**	**0.028**
HC-Deflection-Amp(mm)	**0.92 ± 0.07***	**0.95 ± 0.10**	**0.98 ± 0.10**	**0.021**
A1-Time(ms)	**7.42 ± 0.25**	**7.54 ± 0.27**	**7.52 ± 0.23**	**0.042**
A2-Time(ms)	22.15 ± 0.40	21.99 ± 0.39	21.98 ± 0.48	0.077
SSI	**0.87(0.80,0.93)**	**0.83(0.73,0.89)***	**0.88(0.79,0.97)**	**0.017**
ARTh	**609.43(518.99,663.71)**	**536.46(471.29,625.09)**	**565.83(484.96,658.36)**	**0.028**

**P < 0.05 vs. the PM-PS group. A total of 19 Corvis ST parameters were recorded and analyzed. Parameters without statistically significant between-group differences (SP-A1, DA-Ratio-Max-2mm, Integrated Radius, A1 Velocity, A2 Velocity, HC Time, Whole-Eye Movement Max, and dArcLengthMax) are not shown for brevity; the complete results are provided in Supplementary Table S1*

2.2 Independent effects after adjustment for age, AL and CCT

As presented in Table 3, after adjusting for age, AL and CCT, most statistically significant univariate inter-group differences disappeared, indicating that these disparities were mainly driven by baseline confounders.

The overall inter-group effects remained statistically significant for DA-Ratio-Max-1mm ($F = 4.00$, $P = 0.020$, partial $\eta^2_p = 0.054$), A2-Time (F = 3.38, P = 0.037, partial $\eta^2_p = 0.046$), and Max-InverseRadius (F = 3.33, P = 0.039, partial $\eta^2_p = 0.045$). DA-Ratio-Max-1mm and A2-Time showed a monotonic increasing gradient of MM < SHM < PM-PS. Although crude mean values of A2-Time were comparable among groups and even slightly lower in the PM-PS group, the adjusted mean A2-Time was highest in the PM-PS group (MM: 21.90 ms; SHM: 22.03 ms; PM-PS: 22.28 ms). Adjusted A2-Time was significantly longer in the PM-PS group compared with the MM group (+ 0.379 ms, $P = 0.013$) and the SHM group (+ 0.251 ms, $P = 0.019$). DA-Ratio-Max-1mm was significantly higher in the PM-PS group relative to the MM group (+ 0.036, $P = 0.017$). For Max-InverseRadius, the peak adjusted mean value was observed in the SHM group rather than the PM-PS group, and no statistically significant pairwise post-hoc comparisons were obtained between any two groups. (Fig. 1).

Table 3
Adjusted inter-group effects and estimated marginal means of corneal biomechanical parameters after adjusting for age, AL and CCT

Variable	MM-corrected mean ± SE	SHM-corrected mean ± SE	PM-PS-corrected mean ± SE	F	P	Partial η^2_p
DA-Ratio-Max-1mm	**1.548 ± 0.008***	**1.573 ± 0.005**	**1.583 ± 0.010**	**4.00**	**0.020**	**0.054**
A2 Time (ms)	**21.903 ± 0.077***	**22.030 ± 0.048***	**22.281 ± 0.097**	**3.38**	**0.037**	**0.046**
Max Inverse Radius (mm^-1)	**0.163 ± 0.003**	**0.170 ± 0.002**	**0.165 ± 0.004**	**3.33**	**0.039**	**0.045**
Deflection-Amp-Max(mm)	0.955	0.964	0.96	0.101	0.904	0.001
HC-Deformation-Amp(mm)	1.095	1.105	1.118	0.174	0.84	0.002
HC Deflection Amp. (mm)	0.945 ± 0.018	0.945 ± 0.011	0.949 ± 0.023	0.01	0.989	0.000
A1 Time (ms)	7.475 ± 0.048	7.540 ± 0.030	7.436 ± 0.061	2.08	0.129	0.029
SSI	0.883 ± 0.028	0.835 ± 0.018	0.894 ± 0.036	2.40	0.094	0.033
ARTh	608.158 ± 22.765	560.270 ± 14.278	578.442 ± 28.894	1.79	0.171	0.025

*Estimated marginal means adjusted to the grand mean of covariates. SE = standard error. *P < 0.05 vs. the PM-PS group.*

3. Incremental value of corneal biomechanical parameters for identifying PM-PS

Parameters with P < 0.10 in the univariate comparison were entered into the ROC analysis. When differentiating PM-PS from non-PM-PS eyes, AL, SE, and AL/CR yielded AUC values of 0.894 (95% CI: 0.841–0.948), 0.851 (95% CI: 0.786–0.916), and 0.852 (95% CI: 0.787–0.918), respectively. Individual corneal biomechanical parameters exhibited limited discriminative performance, with all AUC values ≤ 0.646. The highest AUC values were observed for Deflection-Amp-Max (AUC = 0.646), HC-Deformation-Amp (AUC = 0.641), and Peak-Dist (AUC = 0.640). SSI and A2-Time showed promising incremental diagnostic value.

The classical base model (AL + SE) yielded an AUC of 0.896. When single biomechanical indices were added to this base model, no significant ΔAUC was observed; however, meaningful incremental discrimination was detected according to IDI. A2-Time showed IDI = 0.069 (*P* = 0.022) and continuous NRI = 0.770; SSI showed IDI = 0.054 (*P* = 0.014) and continuous NRI = 0.571. Combining A2-Time and SSI into the AL + SE model substantially improved discriminative ability: AUC increased from 0.896 to 0.961 (ΔAUC = 0.065, *P* = 0.005), with IDI = 0.220 (*P* < 0.001) and NRI = 1.341.(Fig. 2).

For Model 2, the baseline clinical model (AL, age, sex, CCT) had an AUC of 0.946. Adding A2-Time alone (ΔAUC = 0.014, *P* = 0.094) or SSI alone (ΔAUC = 0.001, *P* = 0.888) yielded no statistically-significant AUC improvement. Only the combined inclusion of A2-Time and SSI significantly boosted discrimination (AUC = 0.971; ΔAUC = 0.025, *P* = 0.038, IDI = 0.112, NRI = 1.048), providing incremental diagnostic value over the full clinical baseline model.

Table 4
AUC and incremental diagnostic value of parameters and models for distinguishing PM-PS from non-PM-PS eyes.

Variable (N = 147)	**AUC**	**95%CI**	**Cut-off**	**Sensitivity (%)**	**Specificity (%)**
AL(mm)	0.894	0.841–0.948	≥ 26.93	96.9	66.1
SE(D)	0.851	0.786–0.916	≤-8.875	90.3	70.2
AL/CR	0.852	0.787–0.918	≥ 3.43	100	56.1
Deflection Amp. Max	0.646	0.534–0.758	≥ 0.979	65.6	64.9
HC Deformation Amp.	0.641	0.530–0.752	≥ 1.152	56.2	72.8
SSI	0.6	0.488–0.712	≥ 0.880	56.2	61.9
A2-Time(ms)	0.572	0.454–0.690	≤ 22.112	71.9	46.5
Model 1 (N = 147)	AUC	ΔAUC	P	IDI	NRI
Classic(AL + SE)	0.896	-	-	-	-
Classic+A2-Time	0.924	0.028	0.125	0.069	0.77
Classic + SSI	0.907	0.011	0.316	0.054	0.571
Classic+A2-Time + SSI	0.961	0.065	**0.005**	0.220	1.341
Model 2 (N = 147)	AUC	ΔAUC	P	IDI	NRI
Clinical (AL + Age + Sex + CCT)	0.946	-	-	-	-
Clinical +A2-Time	0.959	0.014	0.094	0.034	0.616
Clinical + SSI	0.947	0.001	0.888	0.02	0.667
Clinical +A2-Time + SSI	0.971	0.025	**0.038**	0.112	1.048

AUC = area under the receiver operating characteristic curve; ΔAUC = change in AUC; IDI = integrated discrimination improvement; NRI = net reclassification improvement.

Discussion

In the present study, Corvis-ST data from 147 myopic eyes were analyzed to compare corneal biomechanical profiles among MM, SHM and PM-PS. After adjusting for age, AL and CCT, DA-Ratio-Max-1mm and A2-Time remained independently associated with PS. Notably, a reversal of effect for A2-Time was observed following statistical adjustment. Compared with conventional ocular parameters including AL and SE, individual corneal biomechanical parameters generally exhibited limited discriminatory performance for differentiating PM-PS from non-PM-PS eyes. The basic diagnostic model constructed by AL + SE yielded an AUC of 0.896. When A2-Time and SSI were further incorporated into this AL + SE model, the AUC increased to 0.961 (ΔAUC = 0.065, P = 0.005; IDI = 0.220, P < 0.001; NRI = 1.341), indicating significant improvement in discrimination. These findings suggest that corneal biomechanical parameters provide incremental diagnostic value for identifying PM-PS.

Univariate analysis revealed significant inter-group differences in several biomechanical indices, including Deflection-Amp-Max, Max-InverseRadius, SSI and HC-Deflection-Amp. Corneal deflection amplitude tended to rise

with increasing myopia severity, consistent with the finding of a previous meta-analysis[10]. Corvis-ST studies in Chinese populations also reported a gradual reduction in the SSI as myopia progressed, implying that corneas in highly myopic eyes were more susceptible to deformation[19]. However, after adjustment for age, AL, and CCT, most of these between-group differences were no longer statistically significant. Of note, although CCT was well balanced between groups at baseline, its inclusion in the multivariable model markedly altered the between-group estimates, indicating that the unadjusted differences reflected confounding by these covariates rather than true group-specific effects. These findings highlight that adequate adjustment for key covariates is essential in between-group comparisons of corneal biomechanics, as incomplete adjustment may lead to biased conclusions. (Tables 2 and 3).

After adjustment for age, AL, and CCT, DA Ratio Max 1 mm retained a statistically significant between-group difference ($P = 0.02$, partial $\eta^2 = 0.054$), although the effect size was small to moderate. DA Ratio Max 1 mm is defined as the ratio of the apical deflection amplitude to the deflection amplitude at 1 mm from the corneal apex at maximum indentation; it therefore reflects the central-to-paracentral distribution pattern of corneal deformation rather than the overall magnitude of deflection alone. In our cohort, DA Ratio Max 1 mm increased progressively across the three groups (MM < SHM < PM-PS). Thus, even after adjustment for age, AL, and CCT, eyes with PS showed a distinct central-to-paracentral deformation distribution compared with myopic eyes without staphyloma. That a ratio-based index such as DA Ratio Max 1 mm retained its significance after adjustment, whereas magnitude-based indices such as Deflection Amp Max and SSI did not, is biologically plausible rather than incidental. Magnitude indices are largely determined by the absolute thickness and stiffness of the tissue being deformed and therefore vary strongly with age, AL, and CCT, so that much of their unadjusted between-group difference is absorbed by these covariates. A ratio index, by contrast, internally normalizes the deflection at 1 mm to the apical deflection and thus describes the spatial distribution of deformation rather than its amplitude; it is therefore far less sensitive to the absolute amount of deflection and, consequently, much less dependent on these covariates. In other words, the change in the shape of the deformation response, rather than its magnitude, appears to be the more robust marker of altered corneoscleral mechanics in eyes with PS.

Consistent with this interpretation, a previous large-scale, population-based Corvis ST study in young adults reported a significant association between a DA Ratio parameter and refractive status, with highly myopic eyes showing enhanced corneal responsiveness and altered central-to-paracentral deformation patterns[20]. In vivo evidence further indicates that scleral microstructural and mechanical properties can directly modify the corneal deformation outputs recorded by Corvis ST [21], providing indirect mechanistic support for our findings from the perspective of the integrated corneoscleral complex. Liao et al. [14] likewise reported elevated corneal deformation-related parameters in eyes with PS after adjustment for AL; however, their analysis relied on a binary grouping (presence versus absence of PS), which cannot capture the graded nature of the change. In contrast, we used a three-tiered gradient grouping (MM, SHM, and PM-PS), which allows the evolution of corneal biomechanics along the myopia severity continuum to be delineated more precisely. Vieira et al. [22] also described altered corneal biomechanics in PS subgroup eyes with myopic maculopathy, although the potential influence of key confounders such as age, AL, and CCT was not fully addressed in their analysis.

A2 time, the second applanation time, is defined as the time from the onset of the air puff to the second corneal applanation, and it reflects the overall viscoelastic rebound behaviour of the corneoscleral complex. A reversal of the group effect was observed after adjustment for covariates. In the unadjusted analysis, A2 time did not differ significantly between the three groups, although values showed a non-significant trend toward shortening as

myopia became more severe, consistent with observations from several previous myopia cohorts[23]. After adjustment for age, AL, and CCT, however, this tendency reversed: the adjusted marginal mean A2 time was longest in the PM-PS group (22.28 ± 0.10 ms) and shortest in the MM group (21.90 ± 0.08 ms), with a significant pairwise difference between the two groups (mean difference = 0.38 ms; P = 0.037, partial η^2 = 0.046). Axial elongation exerts an independent shortening effect on A2 time and may therefore mask the influence of PS itself: because AL is greatest in the PM-PS group, its shortening effect counteracts the staphyloma-related prolongation of rebound time, so that the two opposing contributions largely offset each other in the unadjusted comparison. Only when AL is statistically accounted for does the PS-related prolongation of A2 time become apparent. Previous Mendelian randomization studies suggest that corneal biomechanical alterations are not merely passive secondary consequences of axial elongation, and that intrinsic biomechanical properties of the ocular wall may participate in the pathogenesis of pathologic myopia (PM) [24]. This provides circumstantial support for our observation of corneoscleral viscoelastic changes that appear to be independent of AL.

In contrast to the parameters that changed monotonically, Max InverseRadius displayed an inverted U-shaped trajectory (∩), peaking in the SHM group and declining in the PM-PS group. A consistent inverted U-shaped pattern was observed for A1 time, whereas SSI and ARTh showed U-shaped trajectories (∪) with a nadir in the SHM group. These divergent patterns suggest that corneal biomechanical changes are not uniformly progressive as myopia advances. We therefore propose a stress-redistribution mechanism: simple high myopia is characterized by global ocular expansion and reduced overall stiffness, resulting in increased instantaneous corneal bending and thus a higher Max InverseRadius. Once a focal PS develops, intraocular stress is redistributed toward the posterior outpouching region, reducing mechanical loading on the anterior cornea and thereby decreasing instantaneous corneal curvature changes. ((Fig. 1))

Collectively, the coexistence of monotonically increasing indices (DA Ratio Max 1 mm, and A2 Time after adjustment) and non-monotonic, inverted U- and U-shaped indices is consistent with a two-stage remodeling of the ocular wall, in which continuous viscoelastic deterioration and abnormal deformation distribution occur alongside stress redistribution after staphyloma formation. These differentiated biomechanical patterns may reflect a shift from global ocular enlargement to focal posterior structural damage in PM. Nevertheless, several of these trends did not reach statistical significance, and no pairwise difference was found for Max InverseRadius. The proposed stress-redistribution hypothesis requires validation in larger, longitudinal cohorts.

Our results demonstrated that conventional axial-refractive indices (AL, SE, AL/CR) achieved favourable discriminatory performance for PM-PS identification, with AL exhibiting the highest diagnostic efficacy. AL/CR, a composite index combining axial length and corneal curvature, has been applied to evaluate global ocular morphology in axial myopia[25]. Nevertheless, AL/CR failed to demonstrate superiority over AL in our cohort, suggesting that axial length remains the core morphological marker for screening PM-PS. Individual corneal biomechanical parameters generally yielded low AUC values, indicating that no single Corvis-ST-derived metric can independently discriminate PM-PS from non-PM-PS eyes. Corneal deformation responses represent coupled outputs modulated by geometry and material properties under the joint influence of age, AL and CCT, rather than pure intrinsic corneal material properties[26, 27]. Despite limited standalone performance, the combination of SSI and A2-Time delivered promising incremental diagnostic gains. Adding these two biomechanical parameters to the baseline AL + SE model significantly improved discrimination (AUC = 0.971 vs original 0.896, P = 0.005). Even on the clinical baseline model already adjusted for age, sex and CCT (AUC = 0.946), incorporation of SSI plus A2-Time still provided supplementary discriminatory benefit (AUC = 0.971, P = 0.038). Collectively, these results imply that

corneal biomechanical metrics are not suitable for standalone screening of PM-PS, but may serve as valuable adjuncts to conventional axial-refractive parameters to improve PM-PS detection. (Table 4 and Fig. 2)

Several limitations of this study should be acknowledged. First, as a cross-sectional investigation, only correlations can be established; causal-temporal relationships cannot be inferred. It remains undetermined whether corneal biomechanical changes predispose to PS or represent secondary ocular-wall remodelling after staphyloma onset. Second, due to missing data, IOP was not included as a covariate in our analyses, which might introduce bias for Corvis-ST deformation measurements. In addition, the sample size of the PM-PS subgroup was relatively small. Some borderline statistical findings await external validation in larger-scale multicentre myopia cohorts.

Conclusion

Corneal biomechanical differences across myopia severity grades were largely attributable to confounding by age, AL, and CCT. After adjustment, DA Ratio Max 1 mm and A2 time remained independently associated with the presence of PM-PS, and the reversal of the A2 time trend indicates that axial elongation masks the PS-related prolongation of corneal rebound time. Although SSI and A2 time alone showed limited discriminatory power, their combination provided significant incremental value for identifying PM-PS beyond both the classical (AL + SE) and clinical models. Longitudinal studies with larger samples are warranted to validate these findings.

Declarations

Ethics approval and consent to participate:

This prospective study was conducted following the guidelines of the Declaration of Helsinki. This study passed the ethical review of the Tianjin Eye Hospital Medical Science Research Ethics Committee (Approval No. KY2026026). The use of all prospective data in this study was approved with informed consent obtained from all participants.

Consent for publication:

Not applicable.

Competing interests:

None.

Funding:

This work was supported by Tianjin Key Medical Discipline (Specialty) Construction Project (No. TJYXZDXK-016A)

Author Contribution

QHH and XW designed the research. LYR, YW and HZC collected the data. YXB and SYC analyzed the data. YXB drafted the manuscript. XW and YW revised the manuscript. All authors contributed to the article and approved the submitted version.

Acknowledgements:

None.

Data Availability

The data that support the findings of this study are available from the corresponding author upon reasonable request.

References

1. Bullimore MA, Ritchey ER, Shah S, Leveziel N, Bourne RRA, Flitcroft DI. The Risks and Benefits of Myopia Control. Ophthalmology. 2021;128(11):1561–79.
2. Holden BA, Fricke TR, Wilson DA, Jong M, Naidoo KS, Sankaridurg P, et al. Global Prevalence of Myopia and High Myopia and Temporal Trends from 2000 through 2050. Ophthalmology. 2016;123(5):1036–42.
3. Gu SZ, Chang S. Pathologic Myopia. Adv Exp Med Biol. 2025;1467:281–3.
4. Tahhan N, Bullimore MA, He X, Ostrin LA, Gawne TJ, Gifford KL, et al. IMI-2025 Digest. Invest Ophthalmol Vis Sci. 2025;66(12):27.
5. McBrien NA, Gentle A. Role of the sclera in the development and pathological complications of myopia. Prog Retin Eye Res. 2003;22(3):307–38.
6. Li Y, Tan S, Xiong R, Li H, Zhu Z, Chen S et al. Posterior staphyloma and long-term structural and visual trajectories in high myopia. Br J Ophthalmol 2026.
7. Ruiz-Medrano J, Montero JA, Flores-Moreno I, Arias L, García-Layana A, Ruiz-Moreno JM. Myopic maculopathy: Current status and proposal for a new classification and grading system (ATN). Prog Retin Eye Res. 2019;69:80–115.
8. Xu X, Fang Y, Yokoi T, Shinohara K, Hirakata A, Iwata T, et al. POSTERIOR STAPHYLOMAS IN EYES WITH RETINITIS PIGMENTOSA WITHOUT HIGH MYOPIA. Retina. 2019;39(7):1299–304.
9. He M, Wang W, Ding H, Zhong X. Corneal Biomechanical Properties in High Myopia Measured by Dynamic Scheimpflug Imaging Technology. Optom Vis Sci. 2017;94(12):1074–80.
10. Park JH, Choi KR, Kim CY, Kim SS. The height of the posterior staphyloma and corneal hysteresis is associated with the scleral thickness at the staphyloma region in highly myopic normal-tension glaucoma eyes. Br J Ophthalmol. 2016;100(9):1251–6.
11. Komninou MA, Seiler TG, Enzmann V. Corneal biomechanics and diagnostics: a review. Int Ophthalmol. 2024;44(1):132.
12. Liu MX, Zhu KY, Zhu KL. Corneal Biomechanical Characteristics in Myopes and Emmetropes Measured by Corvis ST: A Meta-Analysis. Am J Ophthalmol. 2024;264:154–61.
13. Sun Y, Guo Y, Pang R, Peng J, Cao K, Wang N. Corneal biomechanical properties and potential influencing factors in varying degrees of myopia. Sci Rep. 2024;14(1):20626.
14. Liao X, Yu G, Jiang Y, Zhuang X, Yao S, Li K, et al. The corneal biomechanics of the posterior staphyloma. Photodiagnosis Photodyn Ther. 2026;58:105231.
15. Chu Z, Ren Q, Chen M, Cheng L, Cheng H, Cui W, et al. The relationship between axial length/corneal radius of curvature ratio and stress-strain index in myopic eyeballs: Using Corvis ST tonometry. Front Bioeng Biotechnol.

2022;10:939129.
16. Yang K, Xu L, Fan Q, Zhao D, Ren S. Repeatability and comparison of new Corvis ST parameters in normal and keratoconus eyes. Sci Rep. 2019;9(1):15379.
17. DeLong ER, DeLong DM, Clarke-Pearson DL. Comparing the areas under two or more correlated receiver operating characteristic curves: a nonparametric approach. Biometrics. 1988;44(3):837–45.
18. Pencina MJ, D'Agostino RB, Sr., D'Agostino RB Jr., Vasan RS. Evaluating the added predictive ability of a new marker: from area under the ROC curve to reclassification and beyond. Stat Med. 2008;27(2):157–72.
19. Liu Y, Pang C, Ming S, Fan Q. Effect of myopia and astigmatism deepening on the corneal biomechanical parameter stress-strain index in individuals of Chinese ethnicity. Front Bioeng Biotechnol. 2022;10:1018653.
20. Li DL, Liu MX, Yin ZJ, Li YZ, Ma R, Zheng YJ, et al. Refractive associations with corneal biomechanical properties among young adults: a population-based Corvis ST study. Graefes Arch Clin Exp Ophthalmol. 2024;262(1):121–32.
21. Xie R, Huo Y, Li Y, Qu Z, Zou H, Wang Y. Analysis of In Vivo Sclera Impact on the Biomechanics of Myopic Eyes. Transl Vis Sci Technol. 2025;14(6):8.
22. Vieira BC, Rodrigues D, Heitor J, Coelho J, Sousa P, Lume M, et al. Relationship Between Scheimpflug-Based Ocular Biomechanics and Myopic Maculopathy. Bioeng (Basel). 2026;13(6):658.
23. Kenia VP, Kenia RV, Pirdankar OH. Association between corneal biomechanical parameters and myopic refractive errors in young Indian individuals. Taiwan J Ophthalmol. 2020;10(1):45–53.
24. Li X, Luo S, Lin K, Soha H, Shen M, Lu F, et al. Causal Links Between Corneal Biomechanics and Myopia: Evidence from Bidirectional Mendelian Randomization in the UK Biobank. Bioeng (Basel). 2025;12(4):412.
25. Fan Y, Huang Y, Huang X. Association between Axial Length to Corneal Curvature Radius Ratio and Myopia in Adult Patients. *J Ophthalmol* 2024, 2024:4981095.
26. Miki A, Maeda N, Ikuno Y, Asai T, Hara C, Nishida K. Factors Associated With Corneal Deformation Responses Measured With a Dynamic Scheimpflug Analyzer. Invest Ophthalmol Vis Sci. 2017;58(1):538–44.
27. Ariza-Gracia M, Zurita JF, Piñero DP, Rodriguez-Matas JF, Calvo B. Coupled biomechanical response of the cornea assessed by non-contact tonometry. A simulation study. PLoS ONE. 2015;10(3):e0121486.

Figures



Figure 1. Adjusted means of six Corvis-ST-derived corneal biomechanical parameters in three myopia subgroups. ANCOVA adjusted for age, AL and CCT. MM: mild-to-moderate myopia; SHM: simple high myopia; PM-PS: pathological myopia with posterior staphyloma. Circles indicate adjusted group means; vertical bars show 95% confidence intervals. Significant group differences were present for DA Ratio Max (P = 0.020), A2 Time (P = 0.037), Max Inverse Radius (P = 0.039). Max Inverse Radius and A1 Time demonstrated an inverted U-shaped pattern peaking in the SHM group, whereas SSI and ARTh displayed a U-shaped pattern with their nadir in the SHM subgroup.

Figure 1

Adjusted means of six Corvis-ST-derived corneal biomechanical parameters in three myopia subgroups. ANCOVA adjusted for age, AL and CCT. MM: mild-to-moderate myopia; SHM: simple high myopia; PM-PS: pathological myopia with posterior staphyloma. Circles indicate adjusted group means; vertical bars show 95% confidence intervals. Significant group differences were present for DA Ratio Max (P = 0.020), A2 Time (P = 0.037), Max Inverse Radius (P = 0.039). Max Inverse Radius and A1 Time demonstrated an inverted U-shaped pattern peaking in the SHM group, whereas SSI and ARTh displayed a U-shaped pattern with their nadir in the SHM subgroup.

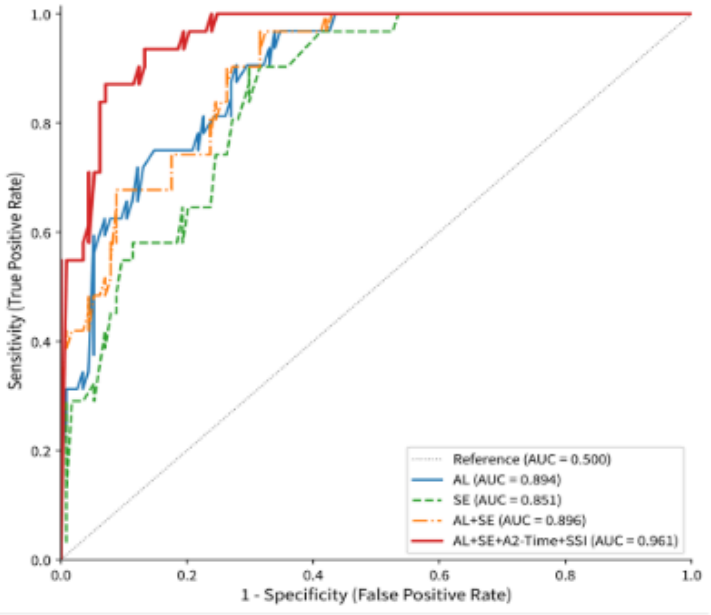


Figure 2. ROC curves for identifying PM-PS from non-PM-PS eyes. The red solid line represents the combined model (AL + SE + A2-Time + SSI, AUC = 0.961); the orange dash-dot line represents the classical model (AL + SE, AUC = 0.896); the blue solid line represents AL alone (AUC = 0.894); the green dashed line represents SE alone (AUC = 0.851). The diagonal dotted line denotes the reference line (AUC = 0.500).

Figure 2

ROC curves for identifying PM-PS from non-PM-PS eyes. The red solid line represents the combined model (AL + SE + A2-Time + SSI, AUC = 0.961); the orange dash-dot line represents the classical model (AL + SE, AUC = 0.896); the blue solid line represents AL alone (AUC = 0.894); the green dashed line represents SE alone (AUC = 0.851). The diagonal dotted line denotes the reference line (AUC = 0.500).

Supplementary Files

This is a list of supplementary files associated with this preprint. Click to download.

- SupplementaryTableS1.xlsx